





RESEARCH PAPER OPEN ACCESS

SorCS2 Is Important for Astrocytic Function in Neurovascular Signaling

Christian Staehr^{1,2} | Hande Login¹ | Elizaveta V. Melnikova¹ | Magdalena Bakun³  | Ewelina Ziemińska⁴ | Lilian Kisiswa¹ | Simin Berenji Ardestani¹ | Stella Solveig Nolte¹ | Hans Christian Beck⁵ | Line Mathilde Brostrup Hansen¹ | Dmitry Postnov⁶ | Alexei Verkhatsky^{7,8,9,10,11}  | Anna R. Malik⁴  | Anders Nykjaer^{1,12,13} | Vladimir V. Matchkov¹ 

¹Department of Biomedicine, Aarhus University, Aarhus, Denmark | ²Department of Anaesthesiology and Intensive Care, Aarhus University Hospital, Aarhus, Denmark | ³Mass Spectrometry Laboratory, Institute of Biochemistry and Biophysics, Polish Academy of Sciences, Warsaw, Poland | ⁴Cellular Neurobiology Research Group, Faculty of Biology, Institute of Developmental Biology and Biomedical Sciences, University of Warsaw, Warsaw, Poland | ⁵Department of Clinical Biochemistry, Odense University Hospital, Odense, Denmark | ⁶Department of Clinical Medicine, Center of Functionally Integrative Neuroscience, Aarhus University Hospital Skejby, Aarhus, Denmark | ⁷Faculty of Biology, Medicine and Health, The University of Manchester, Manchester, UK | ⁸Department of Neurosciences, University of the Basque Country, Leioa, Spain | ⁹IKERBASQUE Basque Foundation for Science, Bilbao, Spain | ¹⁰Department of Forensic Analytical Toxicology, School of Forensic Medicine, China Medical University, Shenyang, China | ¹¹International Joint Research Centre on Purinergic Signalling of Sichuan Province Chengdu University of Traditional Chinese Medicine, Chengdu, China | ¹²PROMEMO and DANDRITE, Aarhus University, Aarhus, Denmark | ¹³Department of Neurosurgery, Aarhus University Hospital Skejby, Aarhus, Denmark

Correspondence: Vladimir V. Matchkov (vvm@biomed.au.dk)

Received: 24 November 2024 | **Revised:** 21 April 2025 | **Accepted:** 22 April 2025

Funding: This work was supported by the Lundbeck Foundation (R344-2020-952 and R412-2022-449 to V.V.M., R90-2011-7723 to A.N. and R248-2017-431 to A.N.), the National Science Centre (OPUS program, 2020/37/B/NZ3/00761; to A.R.M.) and by the Excellence Initiative—Research University, the Action I.3.4, the Programme at the University of Warsaw (A.R.M.), the Danish National Research Foundation (Grant DNRF133 to A.N.) and the Independent Research Fund Denmark—Medical Sciences (3101-00103B to V.V.M. and 7016-00261 to A.N.).

Keywords: astrocytes | calcium signaling | glutamate signaling | neurovascular coupling | SorCS2

ABSTRACT

Introduction: The receptor SorCS2 is involved in the trafficking of membrane receptors and transporters. It has been implicated in brain disorders and has previously been reported to be indispensable for ionotropic glutamatergic neurotransmission in the hippocampus.

Aim: We aimed to study the role of SorCS2 in the control of astrocyte-neuron communication, critical for neurovascular coupling.

Methods: Brain slices from P8 and 2-month-old wild-type and SorCS2 knockout (*Sorcs2*^{-/-}) mice were immunostained for SorCS2, GFAP, AQP4, IB4, and CD31. Neurovascular coupling was assessed in vivo using laser speckle contrast imaging and ex vivo in live brain slices loaded with calcium-sensitive dye. Bulk and cell surface fraction proteomics was analyzed on freshly isolated and cultured astrocytes, respectively, and validated with Western blot and qPCR.

Results: SorCS2 was strongly expressed in astrocytes, primarily in their endfeet, of P8 mice; however, it was sparsely represented in 2-month-old mice. *Sorcs2*^{-/-} mice demonstrated reduced neurovascular coupling associated with a reduced astrocytic calcium response to neuronal excitation. No differences in vascularization or endothelium-dependent relaxation ex vivo between the 2-month-old groups were observed. Proteomics suggested changes in glutamatergic signaling and suppressed calcium signaling in *Sorcs2*^{-/-} brains from both P8 and 2-month-old mice. The increased abundance of glutamate metabotropic receptor 3 in *Sorcs2*^{-/-} astrocytes was validated by PCR and Western blot. In cultured *Sorcs2*^{-/-} astrocytes, AQP4 abundance was increased in the bulk lysate but reduced in the cell surface fraction, suggesting impaired trafficking.

Anna R. Malik, Anders Nykjaer, and Vladimir V. Matchkov contributed equally to this work.

This is an open access article under the terms of the [Creative Commons Attribution-NonCommercial](https://creativecommons.org/licenses/by-nc/4.0/) License, which permits use, distribution and reproduction in any medium, provided the original work is properly cited and is not used for commercial purposes.

© 2025 The Author(s). *Acta Physiologica* published by John Wiley & Sons Ltd on behalf of Scandinavian Physiological Society.

Conclusion: The results suggest that SorCS2 expression is important for the development of neurovascular coupling, at least in part by modulating glutamatergic and calcium signaling in astrocytes.

1 | Introduction

Sortilin Related VPS10 Domain Containing Receptor 2 (SorCS2) is a member of the VPS10P domain family of multi-functional receptors. It participates in cell signaling and mediates trafficking of specific receptors and transporters between intracellular compartments and the plasma membrane to control their surface exposure and activity [1, 2]. The relevance of SorCS2 to human brain disorders has been genetically and/or functionally demonstrated and includes neuropsychiatric diseases, such as schizophrenia [3], bipolar disorder [4, 5], and neurodegenerative conditions, such as Huntington's disease [6] and ischemic stroke [7]. Although the molecular mechanisms underlying the contribution of SorCS2 to these brain pathologies remain incompletely understood, several modalities have been proposed. The expression of SorCS2 is controlled in a temporal manner that is cell-type specific. In particular, SorCS2 is abundant at specific stages of development of the nervous system, where it is indispensable for proper dopaminergic innervation, which may explain its genetic and functional association with neurodevelopmental psychiatric disorders [8]. During adulthood, SorCS2 plays a role in neuronal plasticity by regulating brain-derived neurotrophic factor signaling [6, 9]. It protects against oxidative stress by contributing to the synthesis of glutathione, a key scavenger of reactive oxygen species (ROS) [10]. Hence, SorCS2 deficiency leads to oxidative brain damage, enhanced neuronal cell death, and increased mortality during epilepsy [10]. Whereas SorCS2 is prominent in neurons, its expression in astrocytes in adult mice seems to be low [7, 8, 10, 11]. However, following ischemic stroke, astrocytes upregulate SorCS2, which has been proposed to be important for post-stroke angiogenesis [7].

The survival of neuronal tissue during metabolic challenges depends to a large extent on the efficiency of neurovascular coupling [12]. Neurovascular coupling is essential to match the metabolic demand of neuronal tissues for O₂ and nutrients, and for removal of waste products, which are managed by blood perfusion [13]. Several signaling pathways for neurovascular coupling response were proposed. Although it is still debated [14], some of these pathways implicate astrocytes in transmitting neuronal excitation to local vasodilatation [15–17]. Neuronal firing is sensed by the nearby astrocytes, which respond with intracellular Ca²⁺ waves spreading to the astrocytic endfeet [18–21]. The neuronal activation of astrocytes is mediated by several neurotransmitter receptors, including glutamate receptors present in the plasmalemma of astrocytes [22–24]. Antagonizing N-methyl-D-aspartate (NMDA) receptor or clamping of intracellular Ca²⁺ in astrocytes suppresses neurovascular signaling [16]. As a consequence of astrocyte activation, the endfeet release a plethora of vasoactive substances, leading to relaxation of the adjacent arteriole and an increased blood flow to meet the metabolic demand of the neuronal tissue [25]. Aquaporin-4 (AQP4) is a predominant water channel in the brain that is solely expressed in astrocytes and concentrated in their endfeet [26].

It has been shown that water flux through the AQP4 is important for sustaining K⁺ clearance by astrocytic endfeet upon interstitial K⁺ elevation due to neuronal excitation [27].

Given that SorCS2 expression in astrocytes can be modified under metabolic challenges [7] and that it can regulate NMDA signaling [6, 10, 28], we speculated that SorCS2 may be important for the regulation of neurovascular coupling. We tested our hypothesis by assessing neurovascular coupling in 2-month-old wild-type and SorCS2 knockout (*Sorcs2*^{−/−}) mice in vivo and ex vivo in brain slices. Cerebrovascular function was studied in isolated cerebral arteries. Cerebral vascularization and the capillary–astrocytic endfeet interface were assessed immunohistochemically in 2-month-old brains from wild-type and *Sorcs2*^{−/−} mice. The mechanistic background underlying disturbances in astrocytic function was elucidated using astrocytic bulk and cell surface fraction proteomics followed by ingenuity pathway analysis. The importance of SorCS2 can vary during neuronal development as SorCS2 abundance in astrocytes decreases with maturation of the nervous system [7, 8, 10, 11]. Therefore, to enlighten the potential developmental importance of SorCS2, we assessed whether the changes observed with proteomics are present already in mice at postnatal day 8 (P8). This was further validated by expression analysis in isolated astrocytes from P8 and 2-month-old wild-type and *Sorcs2*^{−/−} mice. This study provides insight into the important role of SorCS2 in neurovascular unit development and function.

2 | Results

2.1 | SorCS2 Is Detected in Astrocytes, but Its Abundance Decreases With Age

Immunohistochemical staining of cerebral cortex in brain slices from eight-day-old (P8) pups revealed strong staining of SorCS2 in GFAP-positive astrocytes surrounding arterioles of wild-type but not *Sorcs2*^{−/−} mice (Figure 1A). The higher magnification images revealed that SorCS2 was abundant in astrocytic aquaporin 4 (AQP4) positive endfeet that encase blood vessel wall and play a critical role in regulation of cerebrovascular resistance (Figure 1B) [16, 17, 19]. Accordingly, an overlapping signal has been detected by double SorCS2 and AQP4 immunolabeling, whereas no signal colocalization has been observed by *Sorcs2* and endothelial marker IB4 double immunolabeling (Figure 1C). No SorCS2 staining was seen in astrocytic endfeet of 2-month-old mice (Figure 2). However, SorCS2 was seen in the astrocytic soma of 2-month-old mice (Figure 2) although to a lesser extent compared to what was observed in P8 pups (Figure 1). Further correlation analysis revealed reduced SorCS2 and GFAP signal overlap in the brain slices from 2-month-old WT mice compared to P8 WT mice (Figure S1). The abundance of SorCS2 outside of the GFAP-positive astrocytes was increased in 2-month-old mice compared to P8 pups (Figures 1 and 2). This suggests an increase

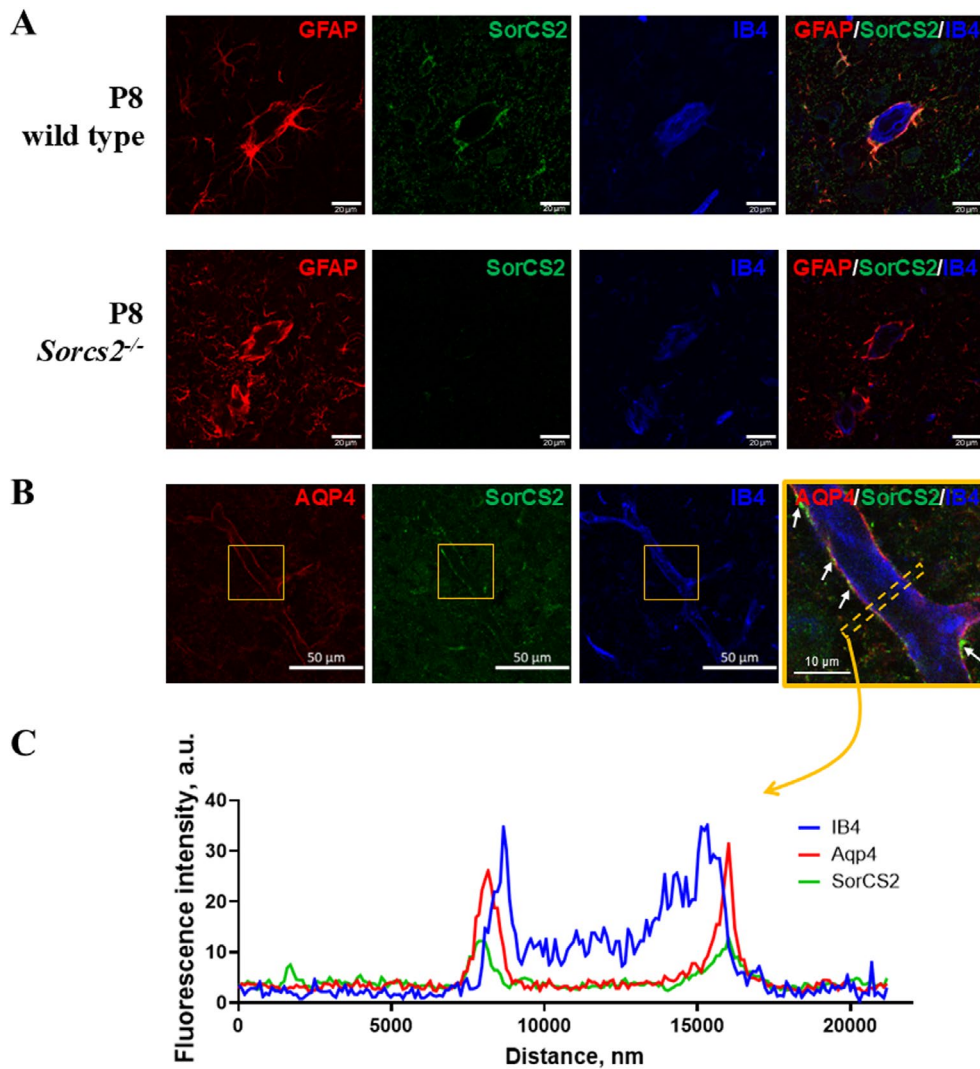


FIGURE 1 | SorCS2 is localized to astrocyte endfeet of newborn mouse brain. In 8-day-old wild-type mice (P8), SorCS2 staining overlapped with the astrocytic marker, glial fibrillary acidic protein (GFAP), and surrounded vascular endothelial cells labeled with α -D-galactosyl-specific isolectin B4 (IB4), as indicated (A). SorCS2-specific staining was not detected in the brain of P8 *Sorcs2*^{-/-} mice, while there was no difference in GFAP and IB4 labeling in *Sorcs2*^{-/-} and wild-type brains (bars correspond to 20 μ m). Representative images for 7 slices from *Sorcs2*^{-/-} mice and for 9 slices from wild-type mice; 2–4 cortical fields of view per slice. The intensive aquaporin-4 (AQP4) and SorCS2 co-labeling suggest that Sorcs2 is localized in the endfeet processes of astrocytes surrounding IB4 positive vascular endothelial cells in the brain of P8 wild-type mice (B; bars correspond to 50 μ m). Merged image suggests an overlap of AQP4 and SorCS2 intensities in astrocytic endfeet in brain slices from P8 wild-type mice, as indicated by arrows in the magnified image (the bar indicates 10 μ m). Two to four cortical fields of view are taken per slice ($n = 9$). The fluorescence intensity profiles over the cross-section, as indicated with a dashed rectangle (B), illustrate an overlay of AQP4 and SorCS2 labeling that is outside of the blood vessel lumen labeled with IB4 (C; the traces representative for P8 brains of 9 wild-type mice).

of SorCS2 expression in neurons with age, as reported previously [7, 8, 10, 11].

2.2 | Reduced Neurovascular Coupling in *Sorcs2*^{-/-} Mice

Neurovascular signaling was measured as relative changes in parenchymal perfusion (Figure 3A,B) of the primary sensory cortex in response to whisker stimulation [29]. The neurovascular responses were assessed in mice anesthetized with ketamine and xylazine and stimulated with mechanical whisker stimulation at 5 Hz for 120 s, as previously [29]. Although anesthesia diminishes neurovascular signaling, this kind of

prolonged mechanical stimulation was previously shown to initiate brain hyperemic responses qualitatively similar to those observed in awake mice with air-puff whisker stimulation [29, 30]. The increase in parenchymal perfusion upon whisker stimulation was reduced in 2-month-old *Sorcs2*^{-/-} mice compared to age-matched wild-type mice (Figure 3C). *Sorcs2*^{-/-} mice exhibited a reduced area of increased parenchymal perfusion (at 6%–11% change in BFI), suggesting impaired propagation of the neurovascular response compared with wild-type mice (Figure S2). Laser speckle contrast imaging was also used to assess changes in arterial blood flow and arterial diameter in response to whisker stimulation (Figure 4A–C). The resting inner diameter of the middle cerebral artery branch supplying the cerebral cortex was similar

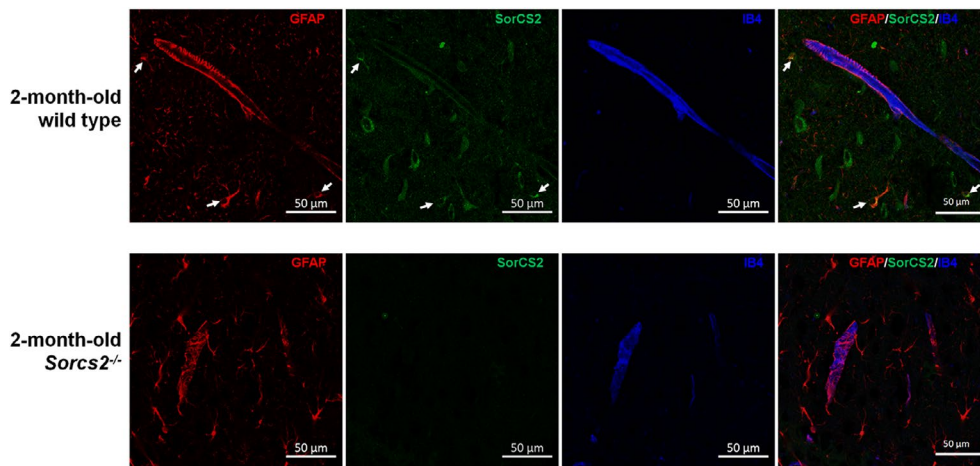


FIGURE 2 | SorCS2 is sparsely detected in astrocytic soma in 2-month-old mouse brain. Brain slices were stained for SorCS2 together with glial fibrillary acidic protein (GFAP) to label astrocytes, and vascular endothelial cell marker α -D-galactosyl-specific isolectin B4 (IB4), as indicated. In 2-month-old wild-type mice, sparse GFAP-SorCS2 co-labeling was detected as indicated by white arrows. No SorCS2 signal was detected in the brain slices from 2-month-old *Sorcs2*^{-/-} mice. Representative images for 2–4 fields of view per slice of 4 slices from *Sorcs2*^{-/-} and 4 slices from wild-type mice. Bars correspond to 50 μ m. See also Figure S1.

in both genotypes (Figure 4D). Whisker stimulation was associated with dilation of this artery, but the vasodilatation observed in 2-month-old *Sorcs2*^{-/-} mice was smaller than in age-matched wild-type mice (Figure 4E). Accordingly, arterial blood flow rise in response to neuronal excitation was reduced in 2-month-old *Sorcs2*^{-/-} mice (Figure 4F).

This suppressed neurovascular coupling was not associated with the changes in brain cortex vascularization of adult *Sorcs2*^{-/-} mice (Figure S3). Although newborn *Sorcs2*^{-/-} pups had slightly elevated vascular density in comparison with age-matched wild types (Figure S3C), this difference was not seen when the brains from 2-month-old *Sorcs2*^{-/-} and wild-type mice were compared (Figure S3D). The sprouting activity was also similar in the brain cortex of *Sorcs2*^{-/-} and wild-type mice when both newborn groups (Figure S3E) and 2-month-old mice (Figure S3F) were compared. There was also no difference in astrocytic endfeet coverage of capillaries in the cortex of 2-month-old *Sorcs2*^{-/-} and wild-type mice (Figure S4A,B). When the distance between astrocytic endfeet and adjacent capillary endothelial cells was compared, no difference between 2-month-old *Sorcs2*^{-/-} and wild-type mice was found (Figure S4C).

2.3 | Neuronal Electric Field Stimulation Elicited the Reduced Intracellular Ca²⁺ Response in Astrocytes From 2-Month-Old *Sorcs2*^{-/-} Mice

Electric field stimulation of brain slices excited neurons and evoked a delayed elevation of intracellular Ca²⁺ in astrocytic endfeet that are clearly distinguished by intense fluorescence surrounding parenchymal arterioles, as shown previously [29, 31–33] (Figure 5A). Electric field stimulation induced a similar elevation of intracellular Ca²⁺ in neuronal tissue but a smaller Ca²⁺ rise in astrocytic endfeet in the cortex brain slices from 2-month-old *Sorcs2*^{-/-} mice compared to age-matched wild-type mice (Figure 5B). The slope of intracellular Ca²⁺ rise was also slower in astrocytes lacking SorCS2 than in wild-type

controls (0.047 ± 0.022 a.u./s versus 0.212 ± 0.039 a.u./s, $n = 4–5$, $p = 0.002$).

2.4 | Similar Endothelial Function in Cerebral Arteries From 2-Month-Old *Sorcs2*^{-/-} and Wild-Type Mice

In accordance with our in vivo measurements (Figure 4D), the inner diameter of relaxed middle cerebral arteries ex vivo was similar between the groups (Figure 6A). To assess the relaxation function, we precontracted the arteries with thromboxane A₂ analog, U46619, to the level of vascular tone corresponding to 80% of their maximal tone and then relaxed the arteries with carbachol. The level of this precontraction was the same for arteries from 2-month-old wild-type and *Sorcs2*^{-/-} mice (0.39 ± 0.08 mN/mm ($n = 11$) versus 0.36 ± 0.03 mN/mm ($n = 8$), $p = 0.69$, for wild-type and *Sorcs2*^{-/-}, respectively). The relaxation by 10^{-5} M carbachol was similar in both groups (Figure 6B). This suggests that the endothelium-dependent vasorelaxation of U46619-precontracted cerebral arteries from 2-month-old *Sorcs2*^{-/-} mice is unchanged in comparison with age-matched wild-type mice.

2.5 | Reduced Glutamatergic Signaling Is Linked to Weakened Astrocytic Ca²⁺ Responses in 2-Month-Old *SorCS2*^{-/-} Mice

Proteomics analyses of isolated astrocytes from P8 WT and *Sorcs2*^{-/-} mice identified overall 3209 proteins (Table S1). Using a cut-off value of $p < 0.05$, it was observed that the abundance of 194 proteins was altered in *Sorcs2*^{-/-} P8 mice ($n = 4$). The abundance of 84 proteins was upregulated, whereas the abundance of 110 proteins was decreased in astrocytes from *Sorcs2*^{-/-} mice (Figure 7A). In astrocytes from 2-month-old mice ($n = 4$), 3668 proteins were identified (Table S2); among them, the abundance of 245 proteins was changed (120 proteins were increased and 125 proteins were decreased in *Sorcs2*^{-/-} mice) (Figure 7B). Of note, False Discovery Rate (FDR) correction in these datasets

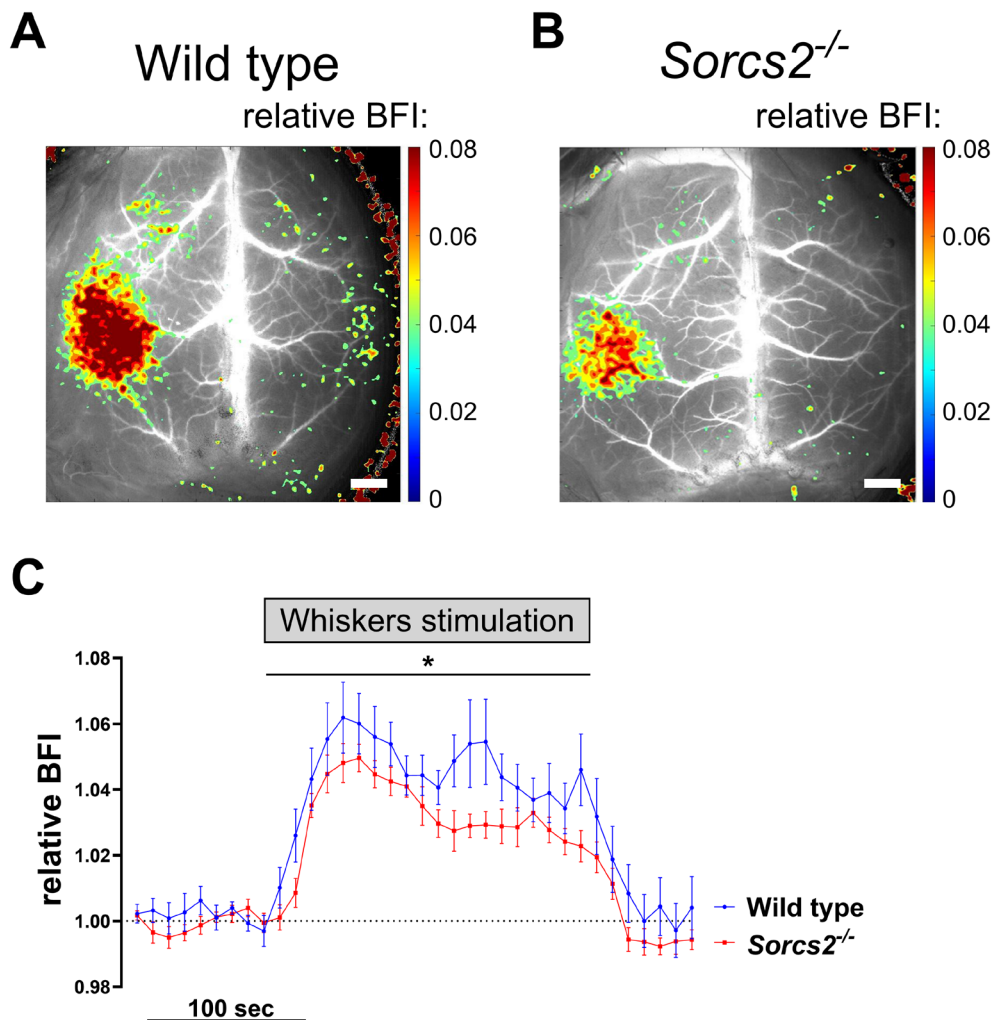


FIGURE 3 | 2-month-old *Sorcs2*^{-/-} mice exhibited reduced neurovascular responses in vivo. An averaged blood flow map (grayscale) with an overlaid relative blood flow index (BFI) changes (color scale) in response to mechanical whisker stimulation, which induced a local change in blood perfusion of the primary somatosensory cortex in age-matched wild-type (A) and *Sorcs2*^{-/-} mice under ketamine and xylazine anesthesia (B). Bars correspond to 1000 μ m. A relative increase in parenchymal BFI of the somatosensory cortex in response to contralateral whisker stimulation was reduced in *Sorcs2*^{-/-} mice ($n=9$) compared to wild-type mice ($n=8$; C). Responses in (C) were compared using two-way ANOVA. * $p < 0.05$. See also Figure S4.

diminishes the statistical power [34, 35]. Only metabotropic glutamate receptor 3 (mGluR3, *grm3*) and RUN domain-containing protein 3B (*Rundc3b*) were found to be significantly changed in astrocytes from 2-month-old *Sorcs2*^{-/-} mice (Table S2). However, the differences in confidential intervals between *Sorcs2*^{-/-} and wild-type mice (Tables S1 and S2) support the differential expression of several proteins as suggested by p values.

Importantly, the abundance of mGluR3 was increased in astrocytes from *Sorcs2*^{-/-} mice of both ages (Table 1; Tables S1 and S2). This increase was the most prominent difference in protein level between the two genotypes in both age groups (Figure 7A,B) and was pronounced with age (Table S2). These results suggest that there might be changes in glutamatergic signaling. This was further validated in isolated astrocytes by mRNA expression analyses of genes that are involved in glutamatergic signaling (Figure 8). The *sorcs2* mRNA expression was diminished in P8 *Sorcs2*^{-/-} isolated astrocytes in comparison with age-matched wild types, while, in accordance with our immunohistochemical results, *Sorcs2* expression was decreased

approximately 7 times in astrocytes from 2-month-old wild-type mice (Figure 8A). In accordance with the results from the proteomics analysis, the increased level of mGluR3 protein was associated with upregulated *grm3* mRNA in isolated astrocytes at both ages of *Sorcs2*^{-/-} mice (Figure 8B). This upregulation was more prominent in 2-month-old mice in comparison with P8 *Sorcs2*^{-/-} mice. Accordingly, our proteomics suggests that both excitatory amino acid transporter 1 (EAAT1) and alanine serine cysteine transporter 1 (ASCT1) were increased in astrocytes from P8 *Sorcs2*^{-/-} mice (Figure S5A and Table S1). The molecular components of glutamatergic signaling underwent more significant remodeling in 2-month-old *Sorcs2*^{-/-} astrocytes, where both AMPA- (GluR2) and NMDA (NMDAR1) receptors were decreased in their abundance (Figure S5B and Table S2). Moreover, the abundance of proteins involved in mitochondrial pathways responsible for glutamate catabolism (i.e., glutamic-oxaloacetic transaminase 2 and glutamate dehydrogenase 1) was reduced (Table S2). Altogether, this suggests that *Sorcs2*^{-/-} astrocytes from 2-month-old mice have modified glutamatergic signaling in comparison with age-matched wild types. This may

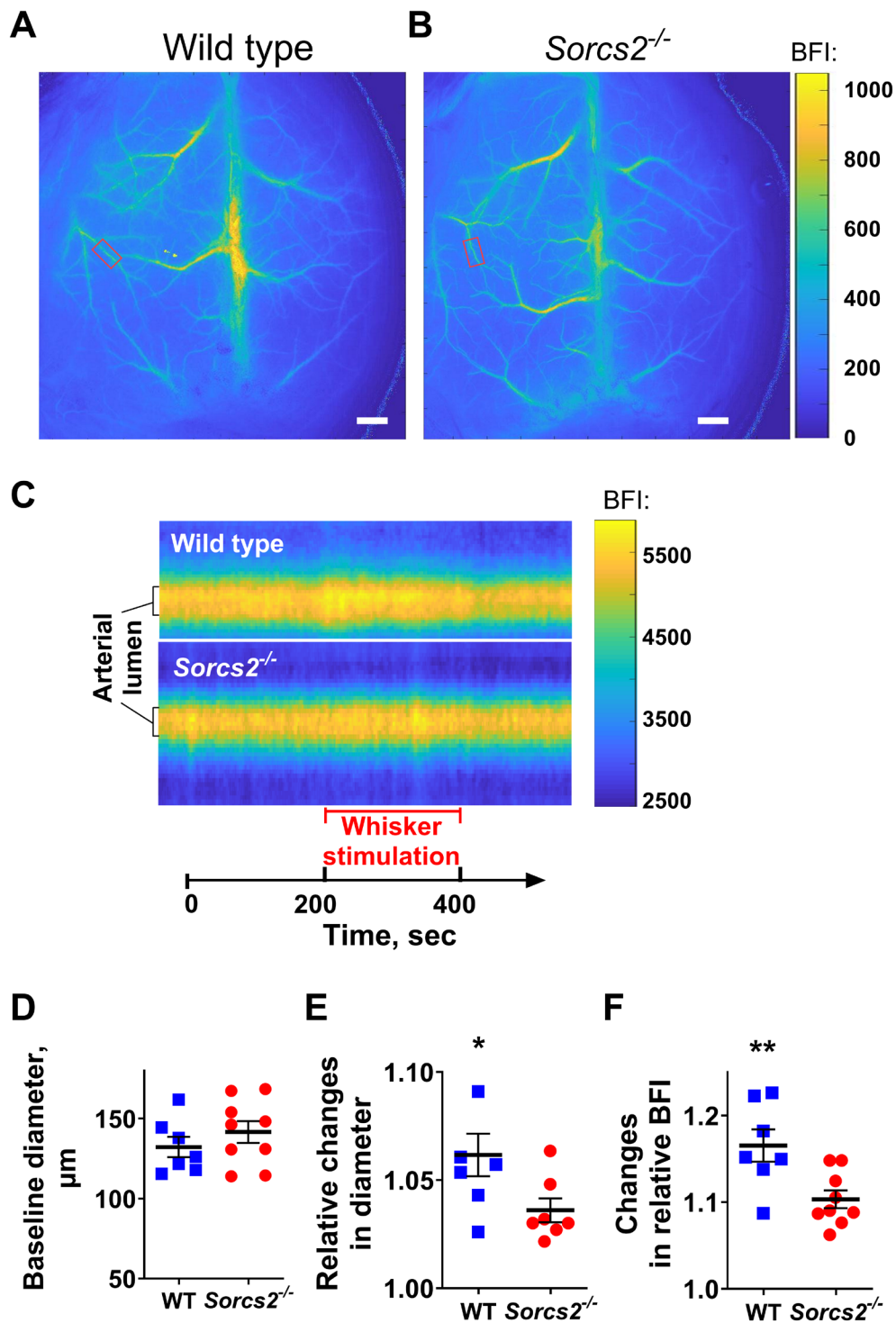


FIGURE 4 | 2-month-old *Sorcs2*^{-/-} mice showed a reduced increase in vascular diameter and blood flow in response to sensory stimulation. Laser speckle contrast imaging was used to assess changes in arterial diameter and arterial blood flow increase in response to whisker stimulation in age-matched 2-month-old wild-type (WT) (A) and *Sorcs2*^{-/-} mice (B). The color scale shows the blood flow index (BFI). Bars correspond to 1000 μm. The red rectangle identifies the 3rd branch of the middle cerebral artery used for single vessel analysis. Representative single artery segmentation profiles show changes in diameter and blood flow in response to whisker stimulation, as indicated on the X-axis (C). Color code corresponds to BFI. The Y-axis indicates a cross-section coordinate with respect to the center of the vessel, i.e., the inner diameter can be identified. There was no difference in baseline diameter of the 3rd branch of the middle cerebral artery between 2-month-old *Sorcs2*^{-/-} and WT mice (D). Averaged peak responses to whisker stimulation revealed that *Sorcs2*^{-/-} mice showed a smaller increase in diameter (E) and blood flow (F) in the 3rd branch of the middle cerebral artery compared to WT. **p* < 0.05 and ***p* < 0.01 (unpaired *t*-test). *n* = 7–9.

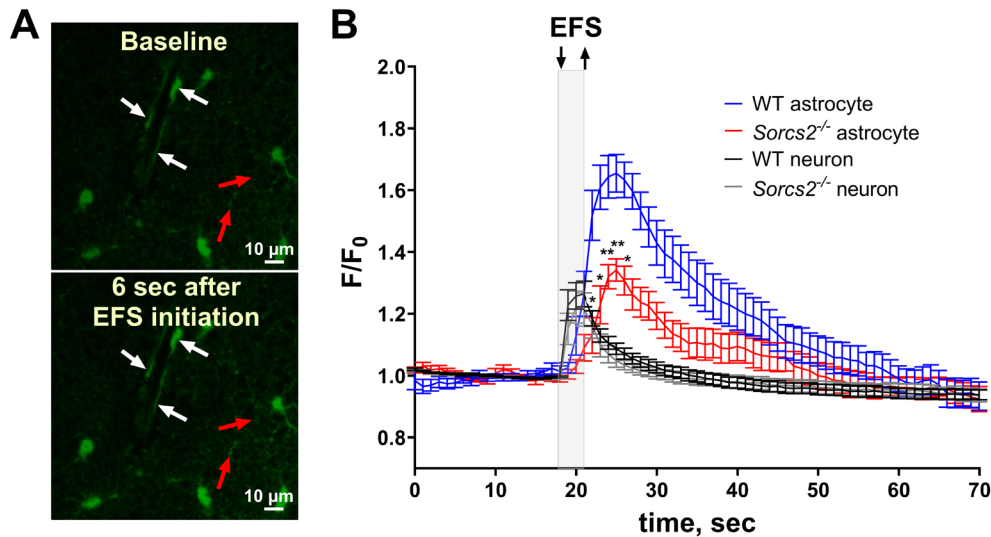


FIGURE 5 | Astrocytes showed a reduced increase in intracellular Ca^{2+} in response to neuronal excitation of the brain slices from 2-month-old *Sorcs2*^{-/-} mice in comparison with age-matched wild types. Brain slices were loaded with Ca^{2+} -sensitive dye, Calcium Green-1/AM. The dye was preferentially allocated to astrocytes and, to a lesser extent, to neuronal tissue (red arrows). White arrows indicate astrocytic endfeet surrounding a parenchymal arteriole (A). Three seconds of electric field stimulation (EFS) increased intracellular Ca^{2+} in astrocytes and neuronal tissue, as shown in representative images from baseline recording and 6 s after initiation of EFS (A). The increase in astrocytic endfeet Ca^{2+} was larger in the brains of 2-month-old wild-type mice ($n = 5$) than in the brain slices from age-matched *Sorcs2*^{-/-} mice ($n = 4$), while no difference in the neuronal Ca^{2+} response was seen (B). $^{**}p < 0.01$ (two-way ANOVA with Sidak's multiple comparisons test).

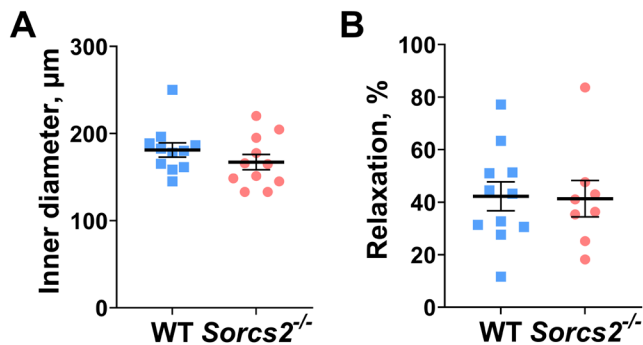


FIGURE 6 | Endothelium-dependent vasorelaxation of the middle cerebral artery was unchanged in 2-month-old *Sorcs2*^{-/-} mice. The diameter of isolated middle cerebral arteries from age-matched wild-type (WT) and *Sorcs2*^{-/-} mice was not different (A). There was no difference in the vasorelaxation in response to 10^{-5} M carbachol between wild-type and *Sorcs2*^{-/-} arteries (B). $n = 8$ –11.

lead to the suppression of neurovascular signaling, as seen in this study in 2-month-old *SorCS2*^{-/-} mice (Figures 3 and 5). This is supported by an increased mRNA expression of GFAP with age in *Sorcs2*^{-/-} mice that was higher in 2-month-old *Sorcs2*^{-/-} astrocytes compared with age-matched control (Figure 8C). The upregulation of GFAP suggests astrocyte remodeling. AQP4 was also found to increase with age, but no difference between genotypes was seen at both the mRNA (Figure 8D) and bulk proteomics level (Tables S1 and S2) between wild types and *Sorcs2*^{-/-} astrocytes matched by mouse age.

As we observed in our functional studies, our proteomics data also implied the reduced intracellular Ca^{2+} signaling in *Sorcs2*^{-/-} astrocytes [19, 20] (Figure 3). This is based on the reduction in Ca^{2+} /calmodulin (CaM)-dependent protein kinase

II (CaMKII) in *Sorcs2*^{-/-} mice at both P8 and 2-month age (Figure S5, Tables S1 and S2). Moreover, the reduction in AMPA- and NMDA receptors may contribute to the suppression of Ca^{2+} influx (Figure S5B and Table S2). Importantly, the reduction of the sarco/endoplasmic reticulum Ca^{2+} -ATPase and endoplasmic reticulum Ca^{2+} binding protein, calreticulin, further supports the suggestion about suppressed intracellular Ca^{2+} signaling in 2-month-old *SorCS2*^{-/-} mice in comparison with age-matched wild types (Figure S5B and Table S2). Hence, proteomics suggested the suppressed expression of the components of glutamatergic signaling and reduced intracellular Ca^{2+} signaling. Changes in these important pathways may have consequences for astrocytic signaling, including neurovascular transmission.

The comparison of the proteomics results obtained from P8 and 2-month-old mice highlighted 13 proteins that were altered in *Sorcs2*^{-/-} mice in both age groups (Figure 7C), but only 7 of them were changed in the same direction in both ages (Table 1). Notably, several of these proteins are known to modulate mitochondrial health and function (Table 1). Accordingly, oxidative phosphorylation was suggested to be diminished in 2-month-old *Sorcs2*^{-/-} mice (Figure S6; Table S3). Although glycerol-3-phosphate dehydrogenase 2 (*gpd2*) mRNA was increased in isolated P8 astrocytes from *Sorcs2*^{-/-}, the 2-month-old mouse astrocytes had a decreased expression of *gpd2* to a similar level (Figure 8E). The proteomics data also proposed changes in intracellular trafficking and protein turnover in astrocytes from *Sorcs2*^{-/-} mice of both ages (Table 1; Table S3). The overall number of canonical pathways, which were suggested to be significantly modified in *Sorcs2*^{-/-} astrocytes and suggested cerebral dysfunctions, increased with age (Figure S6; Table S3). This further supports the idea that the astrocytic phenotype in *Sorcs2*^{-/-} mice changes with age despite the reduced abundance of astrocytic *SorCS2* with maturation of the nervous system.

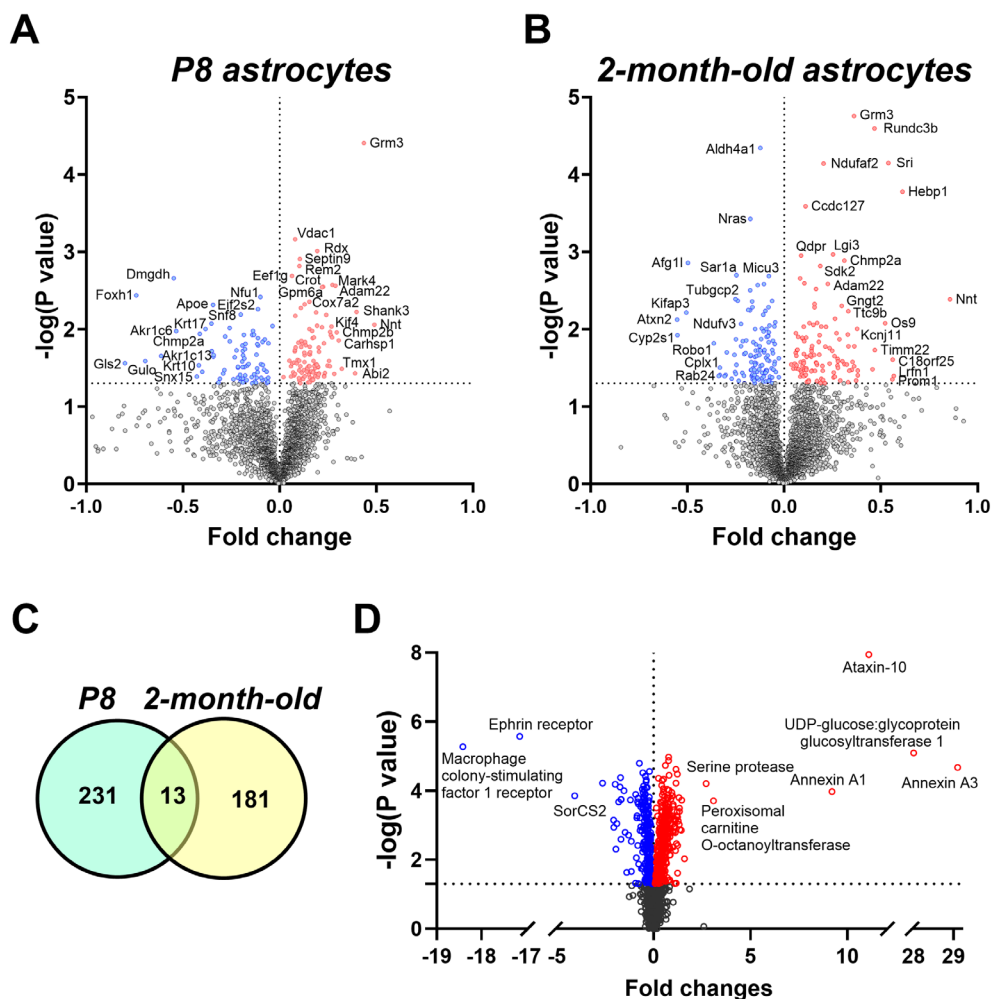


FIGURE 7 | Volcano plot of differentially abundant proteins in astrocytes from wild-type and *Sorcs2*^{-/-} mice. These plots depict fold changes in protein abundance in the lysate of astrocytes from *Sorcs2*^{-/-} versus wild-type mice correlated to the probability that the protein is differentially abundant. Comparisons were made for bulk astrocyte lysates from P8 mice (A) and 2-month-old mice (B). $p < 0.05$ was set as the threshold for differential abundance and depicted on the graphs with a horizontal dotted line. Dots in red denote significantly upregulated proteins, and dots in blue denote significantly downregulated proteins. Gray dots indicate proteins that were not significantly different. Comparisons were made without correction for the False Discovery Rate, although mGluR3 level remains significantly increased after correction. See Tables S1 and S2 for more detailed information. Venn diagram (C) shows the number of proteins, whose abundance was changed in only one of the age groups, i.e., in P8 or 2-month-old mice, and those that were changed in both ages. $n = 4$. Volcano plot of differentially abundant proteins (D) in cell surface fractions of primary *Sorcs2*^{-/-} astrocytes. Comparisons were made without correction for False Discovery Rate. See Table S4 for detailed information; $n = 4$ for (A, B) and $n = 6$ for (D).

TABLE 1 | Differentially expressed proteins, which expression was changed in the same direction in astrocytes from both P8 and 2-month-old *Sorcs2*^{-/-} mice in comparison with wild-type control.

Protein	Abbreviation	SorCS2 ^{-/-} versus WT		Biological function
		P8	2-month-old	
Disintegrin and metalloproteinase domain-containing protein 22	Adam22	1.36	1.25	Synapse formation
Heme-binding protein 1	Hebp1	1.19	1.71	Mitochondrial function
Matrin-3	Matr3	0.83	0.77	Cell differentiation
Metabotropic glutamate receptor 3 (mGluR3)	Grm3	1.58	1.44	Glutamate signaling
Mitochondrial NAD(P) transhydrogenase	Nnt	1.63	2.27	Mitochondrial function
Protein phosphatase 1 regulatory subunit 21	Ppp1r21	1.02	1.10	Endosomal sorting/maturation
Trafficking protein particle complex subunit 10	Trappc10	0.75	0.87	Intracellular trafficking

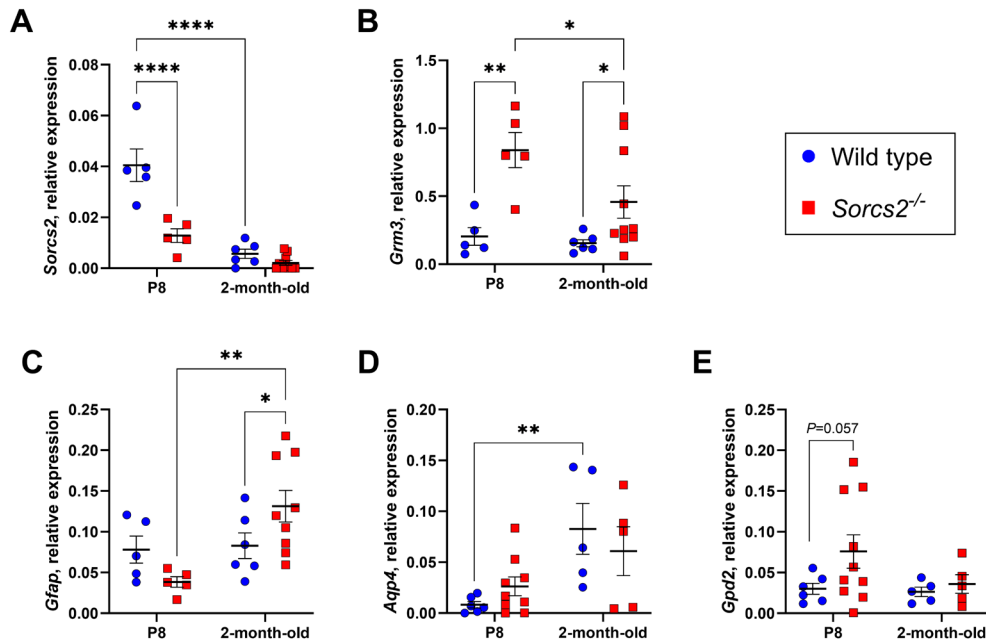


FIGURE 8 | The relative mRNA expression profile of astrocytes from P8 and 2-month-old wild-type and *Sorcs2*^{-/-} mice. (A) P8 *Sorcs2*^{-/-} mice ($n = 5$) have, in comparison with age-matched wild types ($n = 5$), diminished expression of *Sorcs2*. *Sorcs2* expression in astrocytes from 2-month-old wild types ($n = 6$) was suppressed in comparison with P8 wild types. (B) Astrocytes from *Sorcs2*^{-/-} mice showed an increased expression of glutamate metabotropic receptor 3 (mGluR3) mRNA in comparison with age-matched controls at both P8 and 2-month ages. Moreover, mGluR3 expression was lower in astrocytes from 2-month-old than in P8 *Sorcs2*^{-/-} mice. (C) mRNA for glial fibrillary acidic protein (Gfap) was increased in astrocytes from 2-month-old *Sorcs2*^{-/-} mice in comparison with age-matched wild types and P8 *Sorcs2*^{-/-} astrocytes. (D) mRNA for aquaporin-4 (Aqp4) was increased in 2-month-old wild-type mice in comparison with P8 mice. (E) Glycerol-3-phosphate dehydrogenase 2 (Gpd2) mRNA expression had only a tendency for increased expression in P8 *Sorcs2*^{-/-} mice in comparison with age-matched wild type. * $p < 0.05$, ** $p < 0.01$ and **** $p < 0.0001$.

2.6 | Changes in the Cell Surface Fraction Proteins Support Modified Glutamatergic Signaling in *Sorcs2*^{-/-} Astrocytes

Considering the importance of SorCS2 in the trafficking of membrane proteins [1, 2], we performed the proteomics analysis of cell surface fractions of *Sorcs2*^{-/-} and wild-type astrocytes (Table S4, Figure 7D). We found a reduction in several proteins associated with contractile machinery hereof, myosin chains, and neurovascular signaling, e.g., endothelin receptor type B. Furthermore, the reduction in proteins that are important for intracellular Ca^{2+} homeostasis, e.g., the $\text{Na}^+/\text{Ca}^{2+}$ -exchanger, and the Na^+/K^+ -ATPase isoforms, was also evident (Table S4). The abundance of piezo-type mechanosensitive ion channel 1, sarcoplasmic/endoplasmic reticulum Ca^{2+} ATPase 2 (SERCA2), plasma membrane Ca^{2+} -transporting ATPases, and Ca^{2+} /calmodulin-dependent protein kinase type II (CaMKII) was increased in the cell surface fraction (Table S4) that contrasts with bulk proteomics results (Tables S1 and S2). Importantly, the glutamatergic EAAT1 transporter tended to be downregulated in the *Sorcs2*^{-/-} astrocyte membrane (Table S4), although its total abundance was increased in P8 astrocytes (Table S1). Finally, consistent with bulk proteomics and mRNA transcription data, membrane proteomics data suggested an increased GFAP abundance in *Sorcs2*^{-/-} mice (Table S4).

We further validated our findings with Western blot of differentially expressed proteins. Accordingly, the abundance of mGluR2/3 receptor was increased in the cell membrane of

Sorcs2^{-/-} astrocytes (Figure 9). Considering an unchanged AQP4 abundance in bulk proteomics (Tables S1 and S2) and at the mRNA level (Figure 8), its reduced appearance in the membrane (Figure 9) may suggest impaired AQP4 protein trafficking to the membrane in astrocytes from *Sorcs2*^{-/-} mice.

3 | Discussion

This study addressed the importance of astrocytic SorCS2 protein for the integrity of neurovascular coupling. Using conventional SorCS2 knockout mice, we found that SorCS2 deficiency leads to diminished neurovascular signaling in the adult brain. We identified that this was associated with changes in glutamatergic and intracellular Ca^{2+} signaling in astrocytic endfeet from 2-month-old *Sorcs2*^{-/-} mice upon neuronal excitation. Our data suggested that SorCS2 is important for the development of a molecular profile playing a role in astrocytic contribution to neurovascular signal transduction from neurons to parenchymal blood vessels and, thus, explains why *Sorcs2*^{-/-} is associated with disrupted cerebrovascular autoregulation.

3.1 | Temporal Expression of SorCS2 in Astrocytes

SorCS2 has originally been shown to be highly expressed in the mature central nervous system with primary localization to neurons [9]. Previous papers have reported that SorCS2 is only sparsely expressed in astrocytes of healthy adult brains [7, 8, 10].

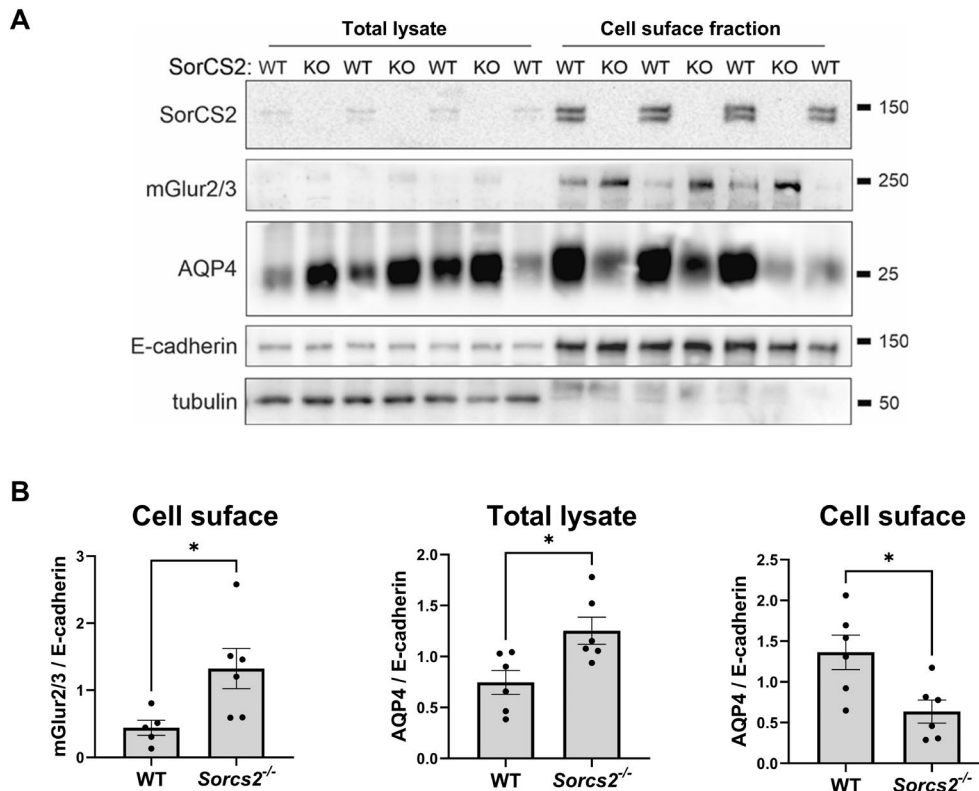


FIGURE 9 | Loss of SorCS2 altered astrocytic cell surface expression of glutamate metabotropic receptors 2 and 3 (mGluR2/3) and aquaporin 4 (AQP4). Primary astrocytes (wild type, WT, and *Sorcs2*^{-/-}, KO) were subjected to a cell surface protein biotinylation assay, and the biotinylated proteins were captured using streptavidin beads prior to Western blot analysis. See also Figure S7 (A) Representative results of Western blot bands of mGluR2/3 receptor (the primary antibody detects both mGluR2 and mGluR3, multimers > 200 kDa)¹⁰ and AQP4 levels in total astrocytic lysates and in cell surface fraction. E-cadherin serves as a loading control and is enriched in the cell surface fraction, while tubulin is depleted from this fraction. SorCS2 is detected in the WT samples. (B) Quantification of the results in (A). Signal intensities for mGluR2/3 and AQP4 were normalized to E-cadherin signals. Graphs show mean ± SEM. *n* = 5–6 biological replicates (independent primary cultures). **p* < 0.05 in two-tailed *t*-test for independent samples.

The present study supports the fact that SorCS2 is expressed to a lesser extent in cortical astrocytes of the adult brain. We found that the astrocytic expression of SorCS2 in P8 mice was particularly high in endfeet, but SorCS2 was not seen in astrocytic endfeet in the brains of 2-month-old mice.

SorCS2 was shown to form the single- and two-chain receptors [8] but also to be present as a homodimer [36]. SorCS receptors may be monomeric, but their dimerization affects their function [36, 37]. It was not technically possible to distinguish between monomer/dimer using Western blot in our experimental settings. Previous studies reported the Western blot bands of 104 kDa and 122 kDa that correspond to the two-chain and one-chain receptors, respectively, as well as a pro-form band at 130 kDa [8]. Accordingly, using the cell surface fractions of primary cultured astrocytes, we identified two bands, which may suggest the pro-form and the single-chain receptor band. We suggest that the two-chain receptor band is not detected as it should migrate to the lower molecular weight [8]. This is in contrast to the previous report that primary cultured neurons express two bands of 104 kDa and 122 kDa [10]. We do not, however, have any direct evidence about the bands' identity and cannot exclude the possibility that these two bands represent a different glycosylated state of the same SorCS2 receptor form.

3.2 | Importance of SorCS2 in Neurovascular Coupling

The high expression of SorCS2 in astrocytic endfeet of P8 mice may suggest that SorCS2 is important in the development of the neurovascular unit [12, 38]. However, the role of changes in receptors and transporters in the neuronal membrane of *SorCS2*^{-/-} adult mice for neurovascular signaling cannot be excluded [9] despite an unchanged neuronal Ca²⁺ response upon electric field stimulation. Neuronal changes were shown previously to have an impact on neurotransmitter release and post-synaptic responses that may influence neuronal connectivity as well as neurovascular coupling [8–10, 28, 39]. Nevertheless, this study was focused on the changes in astrocytic expression and functionality.

Neuronal activity is sensed by astrocytes that express neurotransmitter receptors, including glutamate receptors [22, 23]. Glutamate receptors are localized in the astrocyte membrane in close proximity to neuronal synapses [24], and their activation leads to an increase of intracellular Ca²⁺ that spreads to the astrocytic endfeet wrapping parenchymal arterioles [18–21, 40]. Elevation of intracellular Ca²⁺ in the endfeet initiates a release of substances relaxing arterioles and, thus, increases blood flow to active neurons [41]. Although the role of astrocytic signal

transduction in neurovascular coupling remains controversial [16, 19, 20], we identified the changes in astrocytes that may contribute to the observed reduction of neurovascular signaling in 2-month-old *Sorcs2*^{-/-} mice. Our in vivo measurements demonstrated a reduced propagation of the hyperemic response upon whisker stimulation in *Sorcs2*^{-/-} mice. Proteomics suggested normal astrocytic intercellular communication, as no difference in astrocytic gap junction proteins was detected. Although we have not detected changes in endothelium-dependent relaxation of U46619-precontracted middle cerebral arteries ex vivo, we cannot exclude the possibility of abnormal endothelial function due to global SorCS2 knockout, which can contribute to diminished conductive response as a reason for reduced propagation of neurovascular response in *Sorcs2*^{-/-} mice. As the SorCS2-dependent changes in neuronal circuits cannot be excluded the reduced propagation might be a result of diminished intensity of the original astrocytic response to neuronal excitation, although the contribution of neuronal and endothelial abnormalities cannot be ruled out using the global SorCS2 knockout.

We found a reduction in AMPA and NMDA receptors in astrocytes from 2-month-old *Sorcs2*^{-/-} mice, but SorCS2 is only sparsely expressed in astrocytes at this age. We cannot exclude the importance of SorCS2 for astrocytic glutamatergic receptor and transporters membrane translocation, as it has been shown for the GluN2B subunit of the NMDA receptor in neurons [39]. Accordingly, the membrane translocation of AQP4 was found diminished in this study in *Sorcs2*^{-/-} astrocyte primary culture. The observed changes in the expression profile of *Sorcs2*^{-/-} may be a result of differential neurovascular unit development in wild-type and knockout mice rather than a direct effect of the SorCS2 protein lack in adult astrocytes. However, this hypothesis needs to be validated with inducible knockout, as other studies have shown that SorCS2 directly regulates GluN2B expression in postsynaptic densities and ionotropic synaptic plasticity in the hippocampus, substantiating its importance in controlling neurotransmission [9, 28]. The possible contribution of combined neuronal and astrocytic abnormalities to neurovascular dysfunction in *Sorcs2*^{-/-} mice cannot, therefore, be excluded.

The observed proteomics suggest the changes in activity and astrocytic Ca²⁺ responses [42]. Accordingly, we observed significantly reduced astrocytic Ca²⁺ responses upon neuronal activity, while neuronal Ca²⁺ responses to electric field stimulation were similar between 2-month-old *SorCS2*^{-/-} and wild-type mice. However, as discussed above, this does not exclude the altered neurotransmitter release because of changes in neuronal receptors and transporters *Sorcs2*^{-/-} mice, which might affect astrocytic Ca²⁺ response. The glutamate-triggered Ca²⁺ response in astrocytes depends on a wide spectrum of proteins involved in Ca²⁺ homeostasis [12], including CaMKII [43], which was reduced in *Sorcs2*^{-/-} mice. Furthermore, several Ca²⁺-dependent signaling pathways were predicted to be changed in astrocytes from 2-month-old *Sorcs2*^{-/-} mice, including Ca²⁺ uptake by mitochondria [44] and reduced capacity for storing Ca²⁺ in the sarcoplasmic reticulum [45, 46]. Hence, these changes may be a part of the explanation for the observed reduced Ca²⁺ responses in astrocytes from 2-month-old *Sorcs2*^{-/-} mice. Purinergic signaling was previously proposed to be a component of astrocytic Ca²⁺ transients in neurovascular signaling [17]. The current

study identified only the P2X7 purinoceptor in both bulk and cell surface fraction proteomics but without any changes in its abundance.

Of note, most of the reported proteomics changes in isolated astrocytes are based on *p* values that are not corrected for multiple comparisons due to large datasets that limit the power of statistical analysis [34]. This is supported by differences in the confidence intervals but needs to be interpreted with caution. Some of the proteomics results were validated with quantitative PCR and Western blotting of cell surface fractions, confirming the general direction for the expression profile changes.

To summarize, our data suggest that SorCS2 is necessary for the development of a balanced expression of key astrocytic proteins involved in sensing neuronal activity, i.e., for a proper formation of the neurovascular unit. Whether this is a direct developmental effect in astrocyte ontogenesis or a result of abnormal neuronal function because of SorCS2 knockout remains to be elucidated.

Recent studies have suggested that endothelium is an important component in the neurovascular unit [47]. We observed a reduced neurovascular response to whisker stimulation in 2-month-old *Sorcs2*^{-/-} mice, but ex vivo endothelium-dependent vasorelaxation of U46619-precontracted middle cerebral arteries from 2-month-old *Sorcs2*^{-/-} and wild-type mice was the same. The middle cerebral artery is located upstream for the neurovascular unit that we stimulated with whisker stimulation. Its vasodilatation is, however, important for downstream blood flow rise in response to increased neuronal activity [48]. This retrograde vasodilation is normally conducted through the endothelial cell layer [49], and includes a broad spectrum of signaling pathways [47], where not all of them can be elucidated with carbachol-induced vasodilation of the precontracted artery. Therefore, to exclude the contribution of suppressed endothelial function to conductive vasodilatation, putative endothelial changes in *Sorcs2*^{-/-} mice may further be studied in detail using other means to intervene with multiple endothelial signaling.

3.3 | SorCS2 Knockout Leads to Increased Metabotropic Glutamate Receptor 3 Expression

In astrocytes from both P8 and 2-month-old *Sorcs2*^{-/-} mice, we observed increased expression of metabotropic glutamate receptor 3 (mGluR3). This was seen in the proteomics dataset and validated with PCR and Western blot of astrocytic cell surface fraction. The mGluR3 was previously demonstrated not to be involved in rapid astrocytic Ca²⁺ increases upon neuronal excitation [50]. Nevertheless, the importance of this receptor for modulation of certain neurovascular signaling cannot be excluded. As G_{ai/o}-coupled receptor, mGluR3 is involved in the cAMP signaling that has important implications in some astrocytic responses but was not reported to be important for astrocytic signaling upon sensory stimulation [51]. This is not the first time an increased expression of mGluR3 has been reported in SorCS2 knockout mice [10]. Under physiological conditions, mGluR3 is expressed in astrocytes at all developmental stages [50]. Since mGluR3 activation can potentiate the synthesis of glutathione, it

is protective against oxidative stress [52]. However, our proteomics did not suggest any significant changes in oxidative stress response in astrocytes from P8 or 2-month-old *Sorcs2*^{-/-} mice. The reason and mechanism underlying an increase in mGluR3 in *Sorcs2*^{-/-} mice remain to be investigated.

Other studies reported previously that inhibition of group I metabotropic glutamate receptors, i.e., mGluR1 and mGluR5, suppresses neurovascular coupling [53], although this remains controversial [54]. No such report on the role of mGluR3 is available. However, mGluR3 is known to be upregulated in reactive astrocytes together with mGluR5 [55], but we did not find any expression changes in mGluR1 and mGluR5 in the current study. Importantly, several studies [53, 56, 57] reported that inhibition of NMDA receptors suppresses neurovascular coupling, which is consistent with our findings.

This study used the global constitutive SorCS2 knockout mice as no astrocyte-specific SorCS2 knockout is currently available. This limitation does not allow the exclusion of other extra-brain contributions to observed neurovascular dysfunction in *Sorcs2*^{-/-} mice, e.g., metabolic abnormalities associated with SorCS2 changes. Thus, it has been suggested that SorCS2's importance in glucose-stimulated insulin release [58] may, at least in part, contribute to metabolic disturbances [59] and type 2 diabetes [60]. In fact, *Sorcs2*^{-/-} mice are characterized with normal baseline insulin but blunted response to glucose elevation, suggesting significant fluctuation in blood glucose concentration over time [58]. This glucose fluctuation may lead to astrocyte damage due to mitochondrial dysfunction and impaired glutamate metabolism [61]. Thus, we found in astrocytes from 2-month-old *Sorcs2*^{-/-} mice the reduced proteins involved in mitochondrial pathways responsible for glutamate catabolism, i.e., Got2 [62] and Glud1 [63]. However, no difference in monocarboxylate transporters important for the astrocyte-neuron lactate shuttle was detected [64]. We cannot distinguish with the current experimental setup between the developmental influence of SorCS2 lack in astrocytes and the global contribution of metabolic abnormalities to neurovascular abnormalities in *Sorcs2*^{-/-} mice; however, we demonstrate that the functional SorCS2 is an important determinant of healthy neurovascular development.

3.4 | Neurovascular Uncoupling May Contribute to Neurological Abnormalities Associated With Changes in SorCS2

A previous genome-wide association study suggested that SorCS2 variants increase predisposition to ischemic stroke [65]. Accordingly, SorCS2 polymorphism was shown to be related to the prevalence of ischemic stroke in the Japanese population [66]. The role of SorCS2 in stroke might be linked to its documented role in oxidative stress response protecting neuronal function [10]. Moreover, despite the minimal SorCS2 appearance in healthy astrocytes, it is markedly upregulated after ischemia and contributes to the release of endostatin, a factor linked to post-stroke angiogenesis and neovascularization in the ischemic brain [7]. In this context, the reduction of AQP4 in the cell surface fraction of *Sorcs2*^{-/-} astrocytes is interesting. AQP4 controls water flux between perivascular spaces and

the brain parenchyma and, therefore, is an important player in ischemic and traumatic brain injury edema formation [67]. Since astrocyte-specific AQP4 knockout is protected against post-stroke edema [68], depletion of SorCS2 may improve brain injury outcomes. However, the issue is further complicated by the importance of AQP4 for synaptic plasticity, known to be beneficial for the recovery from brain injury [69]. Further research is needed to elucidate the role of SorCS2-dependent AQP4 membrane translocation in brain injury outcomes.

In the present study, we suggest an additional mechanism that is modulated by SorCS2 and implicated in multiple neuropathological conditions. Disturbance in neurovascular coupling is involved in the pathology of stroke, Alzheimer's disease, migraine, and several other neurodegenerative diseases [12]. Altogether, our results suggest that SorCS2-dependent changes in the development of glutamatergic and Ca²⁺ signaling in astrocytes are important for neurovascular coupling.

4 | Methods

Detailed Methods are available as [Supporting Information](#).

All animal experiments conformed to guidelines from the European Communities Council Directive (86/609/EEC) for the Protection of Animals used for Experimental and other Scientific Purposes. The experiments were conducted with permission from the Animal Experiments Inspectorate of the Danish Ministry of Environment and Food (2016-15-0201-00982 and 2019-15-0201-00341) and reported in accordance with the ARRIVE (Animal Research: Reporting in vivo Experiments) guidelines.

Author Contributions

Christian Staehr: conceptualization, methodology, investigation, writing – original draft, writing – review and editing, formal analysis, visualization, data curation, project administration. **Hande Login:** methodology, investigation, formal analysis, writing – review and editing, visualization, data curation, writing – original draft. **Elizaveta V. Melnikova:** methodology, formal analysis, investigation, writing – review and editing, visualization. **Magdalena Bakun:** methodology, investigation, writing – review and editing. **Ewelina Ziemińska:** methodology, formal analysis, investigation, visualization, writing – review and editing. **Lilian Kisiswa:** methodology, investigation, formal analysis, writing – review and editing. **Simin Berenji Ardestani:** formal analysis, methodology, investigation, writing – review and editing. **Stella Solveig Nolte:** methodology, investigation, visualization, writing – review and editing. **Hans Christian Beck:** methodology, formal analysis, investigation, writing – review and editing. **Line Mathilde Brostrup Hansen:** formal analysis, writing – review and editing. **Dmitry Postnov:** conceptualization, methodology, writing – review and editing, visualization, validation, software, formal analysis, data curation, resources. **Alexei Verkhatsky:** writing – review and editing, supervision. **Anna R. Malik:** conceptualization, writing – review and editing, funding acquisition, formal analysis, methodology, validation, project administration, supervision, resources. **Anders Nykjaer:** conceptualization, funding acquisition, project administration, supervision, validation, resources, writing – original draft, writing – review and editing. **Vladimir V. Matchkov:** supervision, conceptualization, methodology, visualization, project administration, resources, funding acquisition, writing – original draft, writing – review and editing, data curation, formal analysis, validation.

Acknowledgments

We thank Prof. Bozena Kaminska (Nencki Institute of Experimental Biology of the Polish Academy of Science, Poland) for her support. This work was supported by the Lundbeck Foundation [R344-2020-952 and R412-2022-449 to V.V.M., R90-2011-7723 to A.N. and R248-2017-431 to A.N.], the National Science Centre [OPUS program, 2020/37/B/NZ3/00761; to A.R.M.] and by the I.3.4 Action of the Excellence Initiative—Research University Programme at the University of Warsaw [A.R.M.], the Danish National Research Foundation Grant [DNRF133 to A.N.] and the Independent Research Fund Denmark—Medical Sciences [3101-00103B to V.V.M. and 7016-00261 to A.N.].

Conflicts of Interest

The authors declare no conflicts of interest.

Data Availability Statement

The data that supports the findings of this study are available in the [Supporting Information](#) of this article.

References

1. A. R. Malik and T. E. Willnow, “VPS10P Domain Receptors: Sorting out Brain Health and Disease,” *Trends in Neurosciences* 43 (2020): 870–885, <https://doi.org/10.1016/j.tins.2020.08.003>.
2. A. Salasova, G. Monti, O. M. Andersen, and A. Nykjaer, “Finding Memo: Versatile Interactions of the VPS10p-Domain Receptors in Alzheimer’s Disease,” *Molecular Neurodegeneration* 17 (2022): 74, <https://doi.org/10.1186/s13024-022-00576-2>.
3. A. Christoforou, K. A. McGhee, S. W. Morris, et al., “Convergence of Linkage, Association and GWAS Findings for a Candidate Region for Bipolar Disorder and Schizophrenia on Chromosome 4p,” *Molecular Psychiatry* 16, no. 3 (2011): 240–242, <https://doi.org/10.1038/mp.2010.25>.
4. A. E. Baum, N. Akula, M. Cabanero, et al., “A Genome-Wide Association Study Implicates Diacylglycerol Kinase Eta (DGKH) and Several Other Genes in the Etiology of Bipolar Disorder,” *Molecular Psychiatry* 13 (2008): 197–207, <https://doi.org/10.1038/sj.mp.4002012>.
5. H. M. Ollila, P. Soronen, K. Silander, et al., “Findings From Bipolar Disorder Genome-Wide Association Studies Replicate in a Finnish Bipolar Family-Cohort,” *Molecular Psychiatry* 14 (2009): 351–353, <https://doi.org/10.1038/mp.2008.122>.
6. Q. Ma, J. Yang, T. A. Milner, et al., “SorCS2-Mediated NR2A Trafficking Regulates Motor Deficits in Huntington’s Disease,” *JCI Insight* 2, no. 9 (2017): e88995, <https://doi.org/10.1172/jci.insight.88995>.
7. A. R. Malik, J. Lips, M. Gorniak-Walas, et al., “SorCS2 Facilitates Release of Endostatin From Astrocytes and Controls Post-Stroke Angiogenesis,” *Glia* 68 (2020): 1304–1316, <https://doi.org/10.1002/glia.23778>.
8. S. Glerup, D. Olsen, C. B. Vaegter, et al., “SorCS2 Regulates Dopaminergic Wiring and Is Processed Into an Apoptotic Two-Chain Receptor in Peripheral Glia,” *Neuron* 82 (2014): 1074–1087, <https://doi.org/10.1016/j.neuron.2014.04.022>.
9. S. Glerup, U. Bolcho, S. Molgaard, et al., “SorCS2 Is Required for BDNF-Dependent Plasticity in the Hippocampus,” *Molecular Psychiatry* 21 (2016): 1740–1751, <https://doi.org/10.1038/mp.2016.108>.
10. A. R. Malik, K. Szydlowska, K. Nizinska, et al., “SorCS2 Controls Functional Expression of Amino Acid Transporter EAAT3 and Protects Neurons From Oxidative Stress and Epilepsy-Induced Pathology,” *Cell Reports* 26, no. 10 (2019): 2792–2804, <https://doi.org/10.1016/j.celrep.2019.02.027>.
11. V. Kozareva, C. Martin, T. Osorno, et al., “A Transcriptomic Atlas of Mouse Cerebellar Cortex Comprehensively Defines Cell Types,” *Nature* 598 (2021): 214–219, <https://doi.org/10.1038/s41586-021-03220-z>.
12. A. R. Nippert, K. R. Biesecker, and E. A. Newman, “Mechanisms Mediating Functional Hyperemia in the Brain,” *Neuroscientist* 24 (2018): 73–83, <https://doi.org/10.1177/1073858417703033>.
13. C. Iadecola, “Neurovascular Regulation in the Normal Brain and in Alzheimer’s Disease,” *Nature Reviews. Neuroscience* 5 (2004): 347–360.
14. A. Lia, A. Di Spiezio, M. Speggiorin, and M. Zonta, “Two Decades of Astrocytes in Neurovascular Coupling,” *Frontiers in Network Physiology* 3 (2023): 1162757, <https://doi.org/10.3389/fnetp.2023.1162757>.
15. L. Lu, A. D. Hogan-Cann, A. K. Globa, et al., “Astrocytes Drive Cortical Vasodilatory Signaling by Activating Endothelial NMDA Receptors,” *Journal of Cerebral Blood Flow and Metabolism* 39 (2019): 481–496, <https://doi.org/10.1177/0271678X17734100>.
16. A. Institoris, M. Vandal, G. Peringod, et al., “Astrocytes Amplify Neurovascular Coupling to Sustained Activation of Neocortex in Awake Mice,” *Nature Communications* 13 (2022): 7872, <https://doi.org/10.1038/s41467-022-35383-2>.
17. A. Mishra, J. P. Reynolds, Y. Chen, A. V. Gourine, D. A. Rusakov, and D. Attwell, “Astrocytes Mediate Neurovascular Signaling to Capillary Pericytes but Not to Arterioles,” *Nature Neuroscience* 19 (2016): 1619–1627, <https://doi.org/10.1038/nn.4428>.
18. B. L. Lind, A. R. Brazhe, S. B. Jessen, F. C. Tan, and M. J. Lauritzen, “Rapid Stimulus-Evoked Astrocyte Ca²⁺ Elevations and Hemodynamic Responses in Mouse Somatosensory Cortex In Vivo,” *Proceedings of the National Academy of Sciences of the United States of America* 110 (2013): E4678–E4687, <https://doi.org/10.1073/pnas.1310065110>.
19. B. L. Lind, S. B. Jessen, M. Lonstrup, C. Josephine, G. Bonvento, and M. Lauritzen, “Fast Ca(2+) Responses in Astrocyte End-Foots and Neurovascular Coupling in Mice,” *Glia* 66 (2018): 348–358, <https://doi.org/10.1002/glia.23246>.
20. Y. Otsu, K. Couchman, D. G. Lyons, et al., “Calcium Dynamics in Astrocyte Processes During Neurovascular Coupling,” *Nature Neuroscience* 18 (2015): 210–218, <https://doi.org/10.1038/nn.3906>.
21. C. Agulhon, J. Petravic, A. B. McMullen, et al., “What Is the Role of Astrocyte Calcium in Neurophysiology?,” *Neuron* 59 (2008): 932–946, <https://doi.org/10.1016/j.neuron.2008.09.004>.
22. H. R. Parri, T. M. Gould, and V. Crunelli, “Spontaneous Astrocytic Ca²⁺ Oscillations In Situ Drive NMDAR-Mediated Neuronal Excitation,” *Nature Neuroscience* 4 (2001): 803–812, <https://doi.org/10.1038/90507>.
23. J. T. Porter and K. D. McCarthy, “Astrocytic Neurotransmitter Receptors In Situ and In Vivo,” *Progress in Neurobiology* 51 (1997): 439–455.
24. A. N. van den Pol, C. Romano, and P. Ghosh, “Metabotropic Glutamate Receptor mGluR5 Subcellular Distribution and Developmental Expression in Hypothalamus,” *Journal of Comparative Neurology* 362 (1995): 134–150, <https://doi.org/10.1002/cne.903620108>.
25. P. S. Hosford and A. V. Gourine, “What Is the Key Mediator of the Neurovascular Coupling Response?,” *Neuroscience and Biobehavioral Reviews* 96 (2019): 174–181, <https://doi.org/10.1016/j.neubiorev.2018.11.011>.
26. S. Mader and L. Brimberg, “Aquaporin-4 Water Channel in the Brain and Its Implication for Health and Disease,” *Cells* 8, no. 2 (2019): 90, <https://doi.org/10.3390/cells8020090>.
27. M. Amiry-Moghaddam, A. Williamson, M. Palomba, et al., “Delayed K⁺ Clearance Associated With Aquaporin-4 Mislocalization: Phenotypic Defects in Brains of Alpha-Syntrophin-Null Mice,” *Proceedings of the National Academy of Sciences of the United States of America* 100 (2003): 13615–13620, <https://doi.org/10.1073/pnas.2336064100>.
28. J. Yang, Q. Ma, I. Dincheva, et al., “SorCS2 Is Required for Social Memory and Trafficking of the NMDA Receptor,” *Molecular Psychiatry* 26 (2021): 927–940, <https://doi.org/10.1038/s41380-020-0650-7>.
29. C. Staehr, R. Rajanathan, D. D. Postnov, et al., “Abnormal Neurovascular Coupling as a Cause of Excess Cerebral Vasodilation in

- Familial Migraine,” *Cardiovascular Research* 116, no. 12 (2019): 2009–2020, <https://doi.org/10.1093/cvr/cvz306>.
30. C. Staehr, H. Ø. Guldbrandsen, C. Homilius, et al., “Targeting Na,K-ATPase-Src Signaling to Normalize Cerebral Blood Flow in a Murine Model of Familial Hemiplegic Migraine,” *Journal of Cerebral Blood Flow and Metabolism* 45 (2024): 842–854.
 31. O. Peters, C. G. Schipke, Y. Hashimoto, and H. Kettenmann, “Different Mechanisms Promote Astrocyte Ca^{2+} Waves and Spreading Depression in the Mouse Neocortex,” *Journal of Neuroscience* 23 (2003): 9888–9896.
 32. G. K. Povlsen, T. A. Longden, A. D. Bonev, D. C. Hill-Eubanks, and M. T. Nelson, “Uncoupling of Neurovascular Communication After Transient Global Cerebral Ischemia Is Caused by Impaired Parenchymal Smooth Muscle Kir Channel Function,” *Journal of Cerebral Blood Flow and Metabolism* 36 (2016): 1195–1201, <https://doi.org/10.1177/0271678X16638350>.
 33. T. A. Longden, F. Dabertrand, D. C. Hill-Eubanks, S. E. Hammack, and M. T. Nelson, “Stress-Induced Glucocorticoid Signaling Remodels Neurovascular Coupling Through Impairment of Cerebrovascular Inwardly Rectifying K^{+} Channel Function,” *Proceedings of the National Academy of Sciences of the United States of America* 111 (2014): 7462–7467.
 34. D. Pascovici, D. C. Handler, J. X. Wu, and P. A. Haynes, “Multiple Testing Corrections in Quantitative Proteomics: A Useful but Blunt Tool,” *Proteomics* 16 (2016): 2448–2453, <https://doi.org/10.1002/pmic.201600044>.
 35. W. S. Noble, “Mass Spectrometrists Should Search Only for Peptides They Care About,” *Nature Methods* 12 (2015): 605–608, <https://doi.org/10.1038/nmeth.3450>.
 36. D. Janulienė, A. Manavalan, P. L. Ovesen, et al., “Hidden Twins: SorCS Neuroreceptors Form Stable Dimers,” *Journal of Molecular Biology* 429 (2017): 2907–2917, <https://doi.org/10.1016/j.jmb.2017.08.006>.
 37. N. Leloup, L. M. P. Chataigner, and B. J. C. Janssen, “Structural Insights Into SorCS2-Nerve Growth Factor Complex Formation,” *Nature Communications* 9 (2018): 2979, <https://doi.org/10.1038/s41467-018-05405-z>.
 38. C. Iadecola, “The Neurovascular Unit Coming of Age: A Journey Through Neurovascular Coupling in Health and Disease,” *Neuron* 96 (2017): 17–42, <https://doi.org/10.1016/j.neuron.2017.07.030>.
 39. A. Salasova, N. S. Degn, M. Paveliev, et al., “SorCS2 Dynamically Interacts With TrkB and GluN2B to Control Neurotransmission and Huntington’s Disease Progression,” *BioRxiv* (2021): 1–60, <https://doi.org/10.1101/2021.11.03.466767>.
 40. J. Petravic, T. A. Fiocco, and K. D. McCarthy, “Loss of IP3 Receptor-Dependent Ca^{2+} Increases in Hippocampal Astrocytes Does Not Affect Baseline CA1 Pyramidal Neuron Synaptic Activity,” *Journal of Neuroscience* 28 (2008): 4967–4973, <https://doi.org/10.1523/jneurosci.5572-07.2008>.
 41. J. A. Filosa and V. M. Blanco, “Neurovascular Coupling in the Mammalian Brain,” *Experimental Physiology* 92 (2007): 641–646, <https://doi.org/10.1113/expphysiol.2006.036368>.
 42. C. Lecrux and E. Hamel, “Neuronal Networks and Mediators of Cortical Neurovascular Coupling Responses in Normal and Altered Brain States,” *Philosophical Transactions of the Royal Society of London. Series B, Biological Sciences* 371, no. 1705 (2016): 20150350, <https://doi.org/10.1098/rstb.2015.0350>.
 43. X. Zhang, J. Connelly, E. S. Levitan, D. Sun, and J. Q. Wang, “Calcium/Calmodulin-Dependent Protein Kinase II in Cerebrovascular Diseases,” *Translational Stroke Research* 12 (2021): 513–529, <https://doi.org/10.1007/s12975-021-00901-9>.
 44. C. M. Bantle, W. D. Hirst, A. Weihofen, and E. Shlevkov, “Mitochondrial Dysfunction in Astrocytes: A Role in Parkinson’s Disease?,” *Frontiers in Cell and Development Biology* 8 (2020): 608026, <https://doi.org/10.3389/fcell.2020.608026>.
 45. P. B. Simpson and J. T. Russell, “Role of Sarcoplasmic/Endoplasmic Reticulum Ca^{2+} -ATPases in Mediating Ca^{2+} Waves and Local Ca^{2+} -Release Microdomains in Cultured Glia,” *Biochemical Journal* 325, no. Pt 1 (1997): 239–247, <https://doi.org/10.1042/bj3250239>.
 46. M. Ni Fhlathartaigh, J. McMahon, R. Reynolds, et al., “Calreticulin and Other Components of Endoplasmic Reticulum Stress in Rat and Human Inflammatory Demyelination,” *Acta Neuropathologica Communications* 1 (2013): 37, <https://doi.org/10.1186/2051-5960-1-37>.
 47. T. A. Longden and W. J. Lederer, “Electro-Metabolic Signaling,” *Journal of General Physiology* 156 (2024): 156, <https://doi.org/10.1085/jgp.202313451>.
 48. A. Silverman and N. H. Petersen, “Physiology, Cerebral Autoregulation,” in *StatPearls* (StatPearls Publishing, 2023).
 49. T. A. Longden, F. Dabertrand, M. Koide, et al., “Capillary K^{+} -Sensing Initiates Retrograde Hyperpolarization to Increase Local Cerebral Blood Flow,” *Nature Neuroscience* 20 (2017): 717–726, <https://doi.org/10.1038/nn.4533>.
 50. W. Sun, E. McConnell, J. F. Pare, et al., “Glutamate-Dependent Neuroglial Calcium Signaling Differs Between Young and Adult Brain,” *Science* 339 (2013): 197–200, <https://doi.org/10.1126/science.1226740>.
 51. Y. Oe, X. Wang, T. Patriarchi, et al., “Distinct Temporal Integration of Noradrenaline Signaling by Astrocytic Second Messengers During Vigilance,” *Nature Communications* 11 (2020): 471, <https://doi.org/10.1038/s41467-020-14378-x>.
 52. A. Berent-Spillon and J. W. Russell, “Metabotropic Glutamate Receptor 3 Protects Neurons From Glucose-Induced Oxidative Injury by Increasing Intracellular Glutathione Concentration,” *Journal of Neurochemistry* 101 (2007): 342–354, <https://doi.org/10.1111/j.1471-4159.2006.04373.x>.
 53. C. Lecrux, X. Toussay, A. Kocharyan, et al., “Pyramidal Neurons Are “Neurogenic Hubs” in the Neurovascular Coupling Response to Whisker Stimulation,” *Journal of Neuroscience* 31 (2011): 9836–9847, <https://doi.org/10.1523/JNEUROSCI.4943-10.2011>.
 54. N. Calcinaghi, R. Jolivet, M. T. Wyss, et al., “Metabotropic Glutamate Receptor mGluR5 Is Not Involved in the Early Hemodynamic Response,” *Journal of Cerebral Blood Flow and Metabolism* 31 (2011): e1–e10, <https://doi.org/10.1038/jcbfm.2011.96>.
 55. E. Aronica, E. A. van Vliet, O. A. Mayboroda, D. Troost, F. H. da Silva, and J. A. Gorter, “Upregulation of Metabotropic Glutamate Receptor Subtype mGluR3 and mGluR5 in Reactive Astrocytes in a Rat Model of Mesial Temporal Lobe Epilepsy,” *European Journal of Neuroscience* 12 (2000): 2333–2344, <https://doi.org/10.1046/j.1460-9568.2000.00131.x>.
 56. X. Wang, N. Lou, Q. Xu, et al., “Astrocytic Ca^{2+} Signaling Evoked by Sensory Stimulation In Vivo,” *Nature Neuroscience* 9 (2006): 816–823, <https://doi.org/10.1038/nn1703>.
 57. G. C. Petzold, D. F. Albeanu, T. F. Sato, and V. N. Murthy, “Coupling of Neural Activity to Blood Flow in Olfactory Glomeruli Is Mediated by Astrocytic Pathways,” *Neuron* 58 (2008): 897–910, <https://doi.org/10.1016/j.neuron.2008.04.029>.
 58. O. Kalnytska, P. Qvist, S. Kunz, T. Conrad, T. E. Willnow, and V. Schmidt, “SORCS2 Activity in Pancreatic Alpha-Cells Safeguards Insulin Granule Formation and Release From Glucose-Stressed Beta-Cells,” *iScience* 27 (2024): 108725, <https://doi.org/10.1016/j.isci.2023.108725>.
 59. S. B. Lee, J. E. Choi, K. W. Hong, and D. H. Jung, “Genetic Variants Linked to Myocardial Infarction in Individuals With Non-Alcoholic Fatty Liver Disease and Their Potential Interaction With Dietary Patterns,” *Nutrients* 16 (2024): 602, <https://doi.org/10.3390/nu16050602>.
 60. Y. H. Suh, Y. Kim, J. H. Bang, et al., “Analysis of Gene Expression Profiles in Insulin-Sensitive Tissues From Pre-Diabetic and Diabetic

Zucker Diabetic Fatty Rats,” *Journal of Molecular Endocrinology* 34 (2005): 299–315, <https://doi.org/10.1677/jme.1.01679>.

61. A. Quincozes-Santos, L. D. Bobermin, A. M. de Assis, C. A. Gonçalves, and D. O. Souza, “Fluctuations in Glucose Levels Induce Glial Toxicity With Glutamatergic, Oxidative and Inflammatory Implications,” *Biochimica et Biophysica Acta - Molecular Basis of Disease* 1863 (2017): 1–14, <https://doi.org/10.1016/j.bbadis.2016.09.013>.

62. J. Rose, C. Brian, A. Pappa, M. I. Panayiotidis, and R. Franco, “Mitochondrial Metabolism in Astrocytes Regulates Brain Bioenergetics, Neurotransmission and Redox Balance,” *Frontiers in Neuroscience* 14 (2020): 536682, <https://doi.org/10.3389/fnins.2020.536682>.

63. F. Frigerio, M. Karaca, M. De Roo, et al., “Deletion of Glutamate Dehydrogenase 1 (Glud1) in the Central Nervous System Affects Glutamate Handling Without Altering Synaptic Transmission,” *Journal of Neurochemistry* 123 (2012): 342–348, <https://doi.org/10.1111/j.1471-4159.2012.07933.x>.

64. D. Roosterman and G. S. Cottrell, “Astrocytes and Neurons Communicate via a Monocarboxylic Acid Shuttle,” *AIMS Neuroscience* 7 (2020): 94–106, <https://doi.org/10.3934/Neuroscience.2020007>.

65. R. C. Kaplan, A. K. Petersen, M. H. Chen, et al., “A Genome-Wide Association Study Identifies Novel Loci Associated With Circulating IGF-I and IGFBP-3,” *Human Molecular Genetics* 20 (2011): 1241–1251, <https://doi.org/10.1093/hmg/ddq560>.

66. M. Oguri, t. Nagahiro, H. Kamiya, et al., “Association of a Polymorphism of ROR2 and Ischemic Stroke in Japanese Individuals With Chronic Kidney Disease,” *Experimental and Therapeutic Medicine* 1, no. 2 (2010): 377–384, https://doi.org/10.3892/etm_00000059.

67. Q. M. Alhadidi, G. A. Bahader, O. Arvola, P. Kitchen, Z. A. Shah, and M. M. Salman, “Astrocytes in Functional Recovery Following Central Nervous System Injuries,” *Journal of Physiology* 602 (2024): 3069–3096, <https://doi.org/10.1113/JP284197>.

68. N. N. Haj-Yasein, G. F. Vindedal, M. Eilert-Olsen, et al., “Glial-Conditional Deletion of Aquaporin-4 (Aqp4) Reduces Blood-Brain Water Uptake and Confers Barrier Function on Perivascular Astrocyte Endfeet,” *Proceedings of the National Academy of Sciences of the United States of America* 108 (2011): 17815–17820, <https://doi.org/10.1073/pnas.1110655108>.

69. H. E. Scharfman and D. K. Binder, “Aquaporin-4 Water Channels and Synaptic Plasticity in the Hippocampus,” *Neurochemistry International* 63 (2013): 702–711, <https://doi.org/10.1016/j.neuint.2013.05.003>.

Supporting Information

Additional supporting information can be found online in the Supporting Information section.